Platoon Dynamics on Signal Controlled Arterials

PANOS G. MICHALOPOULOS and VIJAY PISHARODY

University of Minnesota, Minneapolis, Minnesota

Car path, platoon length, and flow rate equations are developed for the purpose of studying the platoon dynamics at signalized traffic links. The basic modeling is macroscopic in nature and is based on the formation of shock waves generated within the link due to the intermittent service of traffic by the signals. The analysis reveals not only platoon dispersion but also platoon compression, a phenomenon already observed but not previously described mathematically. It is demonstrated that compression does not only occur to platoons entering the link in red but also to those entering in green even in the absence of a downstream signal. Numerical examples are also presented for demonstrating the applicability of the theory.

INTRODUCTION

Coordination of signals is one of the most complex problems in traffic engineering practice. The efficiency of a coordination scheme depends largely on the traffic model employed for describing the movement of cars (or of the platoons) in signalized links. Ideally best coordination is obtained when the head of the platoon released at the start of green upstream, arrives at the downstream stop line concurrently with the dissipation of the queue at this line.[2, 3] Thus the coordination problem requires prediction of the platoon's head travel time as well as the dissipation time of the downstream queue. Although several models are available for the latter,[3, 13, 14] relatively little is known about platoon behavior.

In the early models (still in use today) an average constant speed within the link is assumed for predicting travel times. Platoon dispersion models were subsequently introduced in order to improve coordination. These models are based on the observation that platoons do not remain

Transportation Science
Vol. 14, No. 4, November 1980

0041-1655/80/1404-0365 $01.25

in a compact state but they tend to diffuse as they move away from the point of their formation. Although the numerous models available[1, 5, 9-12] can predict platoon diffusion, they fail to describe the reverse process frequently observed in signalized traffic links, namely platoon compression. This phenomenon is generally caused by dense flow and density conditions along the highway and it can easily be visualized at traffic bottlenecks (such as signals). Thus, as the platoon enters an area of lower density it tends to diffuse and, conversely, at higher densities it is compressed. High and low density areas are formed within a signalized traffic link not only at the downstream end of it but also upstream due to the different flows released during each phase of the upstream signal.

In this paper new traffic models are presented which exhibit both platoon diffusion as well as compression. The theory is based on an earlier study[8] on macroscopic modeling of traffic flow at signal controlled traffic links. In this work the existence and behavior of shock waves generated periodically downstream and upstream of a traffic signal was demonstrated and analytical expressions were developed for describing their propagation along the road. From these results analytical expressions are derived for describing the paths of any arbitrarily specified mass of vehicles, such as the platoon head and tail. Naturally, these paths are functions of the demands, the link capacity and the signal control policy. The distance between the platoon head and tail (defined here as the platoon length) is further analyzed as the platoon moves along the link in order to identify the time intervals of expansion and compression. Finally, analytical expressions are presented describing the flow rates as a function of time at any point downstream of the signal along with numerical examples illustrating both diffusion and compression. This latter manifestation is of particular importance since it demonstrates that, although the proposed models have not been compared as yet with real data, they appear, in principle, to resemble actual traffic behavior more realistically.

BACKGROUND

CONSIDER THE INTERSECTION of two N-S, E-W streets as shown in Figure 1. Without loss of generality assume that the major flow of traffic occurs in the W to E direction and that no traffic sinks or sources are present downstream of the intersection. Further, consider the traffic link beginning at $B'B$ and initially suppose that no signal or other control devices exist at the downstream end of it. This latter assumption can easily be removed and the effects of a downstream signal can be taken into account.[8]

Since no entrances or exists are present within the link under consid-

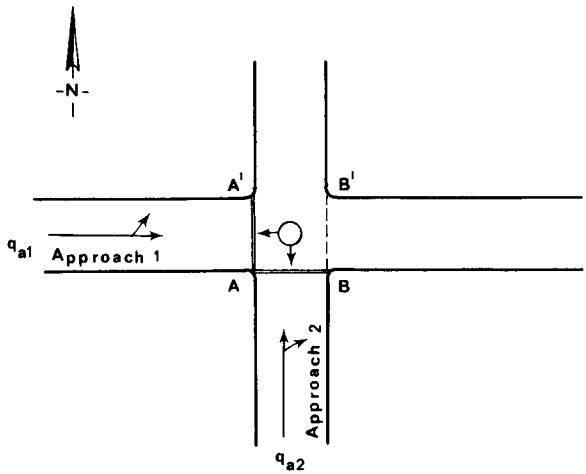

Fig. 1. Upstream end of link.

eration the law of conservation applies, resulting in the equation of continuity:

$$\partial q/\partial x + \partial K/\partial t = 0 \tag{1}$$

where q, K represent flow rate and density and x, t, space and time, respectively. If flow is a function of density, i.e., if $q = f(K)$, solution of the continuity equation can be obtained by the method of characteristics as suggested by LIGHTHILL AND WHITHAM.[7] Briefly, the solution suggests that density at any point of the time-space domain can be found graphically by drawing straight lines called "characteristics." The characteristics emanate from the boundaries of the time-space domain and they carry the value of density defined at these boundaries (known as initial and boundary conditions). If d represents the link length and $n \cdot c$ the period of n cycles, then initial conditions represent the value of density along the x axis ($0 \leq x \leq d$) at $t = 0$; similarly, boundary conditions represent the value of density along the t axis ($0 \leq t \leq nc$) at $x = 0$. Initial and boundary conditions must be defined from physical considerations. Once these conditions are defined then the slope of the characteristic lines (emanating from the boundaries) is the same as that of the tangent to the flow versus concentration curve evaluated at the point defined by the q, K values corresponding to the origin of the characteristic. When two characteristic lines intersect, density at the point of intersection should have two values but this is physically unrealizable. The discontinuity of density at this point is explained by the

generation of a shock wave which moves backward or forward with respect to the highway with speed u_w given by

$$u_w = (q_d - q_u)/(K_d - K_u) \tag{2}$$

where q_d, K_d and q_u, K_u represent the flow and density conditions downstream and upstream of the point of intersection. A number of models expressing flow as a function of density with various degrees of success are available (see for example GERLOUGH et al.[4]). For simplicity the GREENSHIELDS[6] model is used throughout this paper but it should be noted that analogous results can be obtained by similar analysis for any other flow-density relationship. Thus from the assumed flow-density relationship Eq. 2 becomes

$$u_w = u_f(K_j - K_d - K_u)/K_j \tag{3}$$

where u_f and K_j represent the free flow speed and jam density, respectively.

The discussion to this point suggests that, in order to describe the traffic dynamics within the link downstream of line $B'B$ (Fig. 1), initial and boundary conditions must be defined. Before this is accomplished, however, it is essential to examine the traffic arrivals at the boundary $B'B$. Naturally, these arrivals are related to the departures from the stop lines $A'A$ and AB and are time varying. An exact description of the arrival patterns (which depend on the particular intersection) is difficult to obtain due to the stochastic nature of the arrivals and the turning movements at the intersection. Thus, for simplicity an average arrival flow rate $q_i^{(n)}$, per phase i during the nth cycle is assumed on line $B'B$. The arrival rates can of course vary from cycle to cycle and they are functions of the signal timing, the saturation flow on each approach, the turning movements, and the intersection demands. Assuming a two phase operation, q_1 and q_2 can be estimated. Analytical expressions approximating q_1 and q_2 can be found in MICHALOPOULOS et al.[8] It should be pointed out that although the assumption of an average flow rate per phase is a simplification of real world conditions it offers an improvement over recently proposed models[2, 11] in which a constant average flow rate during the entire cycle is assumed.

The flow conditions q_1 and q_2 correspond to average densities K_1 and K_2 at the upstream end of the link (line $B'B$, at which $x = 0$). Without loss of generality it can be assumed that the flow q_1 released during the main street green interval g_1 is greater than the flow q_2 released during the red interval r_1; otherwise the analysis is not affected but the phase notation should be reversed. The intervals g_1 and r_1 correspond to the

effective green and red times as defined by WEBSTER[14] and are such that in every cycle $g_1 + r_1 = c$ where c represents the cycle length.

From q_1 and q_2 the densities K_1 and K_2 can be obtained depending on the flow-density relationship one is willing to accept. For example from Greenshields model[6] it can be easily verified that K_1 and K_2 are given by

$$K_i = (1/2)[K_j - (K_j^2 - 4K_j q_i/u_f)^{1/2}], \quad i = 1, 2 \tag{4}$$

where K_j and u_f are the jam density and the free flow speed of the W-E road. Since $q_1 > q_2$ and both flows correspond to uncongested conditions it follows that $K_1 > K_2$. Thus at the boundary $x = 0$ flow and density conditions change periodically from $q_1^{(n)}$, $K_1^{(n)}$, to $q_2^{(n)}$, $K_2^{(n)}$.

Having defined the density conditions at the boundary $x = 0$ the characteristic lines can be drawn. This is accomplished in Figure 2 for three consecutive cycles. As the figure suggests the slope of the characteristic lines emanating from the t axis during the green intervals is $h(K_1)$ which is the same as that of the tangent to point 1 of the flow-density curve shown in the upper left corner of the figure. The characteristic lines during the red intervals have higher slope $h(K_2)$ and they are drawn similarly. Finally, in each cycle at the beginning of the effective green

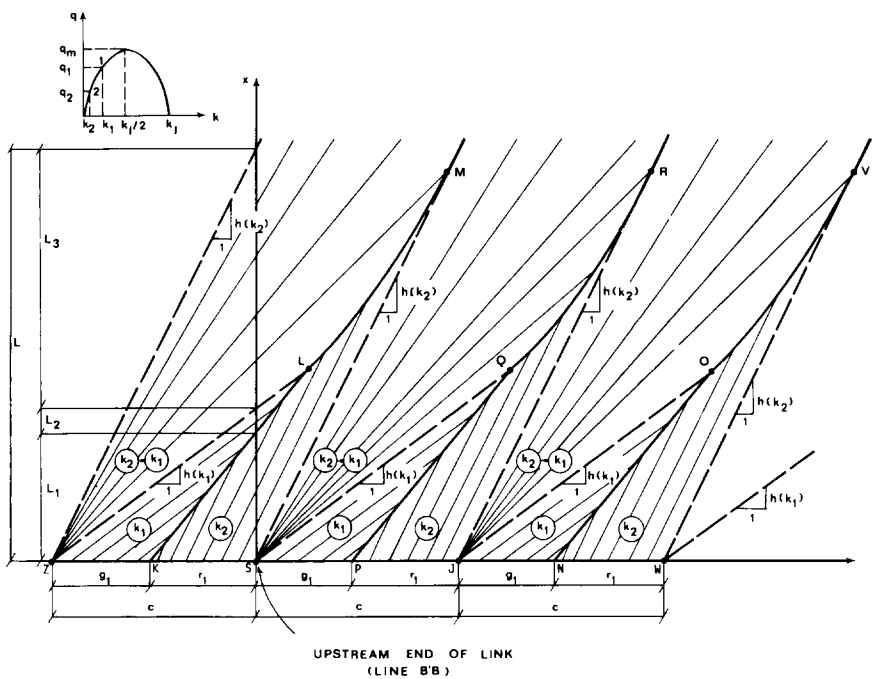

Fig. 2. Shock wave developments downstream of line $B'B$.

density changes instantaneously from K_2 to K_1 implying that the characteristics "fan out" i.e., their slopes take on all possible values from $h(K_2)$ to $h(K_1)$. Therefore these characteristics carry densities in the range $[K_2, K_1]$. The intersection of the characteristics at the beginning of the effective red interval results in shock waves *KLM*, *PQR*, *NOV* etc. (Fig. 2) which propagate downstream of the highway (i.e., downstream of line $B'B$ in Fig. 1). When the characteristics on each side of a shock wave are of constant slope, shock wave speed, given by Eq. 2, is constant and its trajectory is a straight line; otherwise the shock waves propagate with variable speed and their trajectories are nonlinear. For example, shock wave *PQR* consists of three distinct segments *PQ*, *QR* and the segment beyond *R*. The first (*PQ*) is a straight line as densities on both sides of the shock wave are constant; the second (*QR*) is a curve since density is variable downstream of the shock wave, and the last segment (beyond *R*) is also a curve with variable density on both sides. Returning to Fig. 2 it is noted that the dashed lines *SM*, *SQ*, *JR*, etc. represent the last characteristics carrying density K_2, K_1, K_2, etc. and they separate the various zones having different density properties. Finally, it should be remembered that the characteristics do not represent the trajectories of cars but rather the propagation of a flow and density condition along the highway, and they are frequently referred to as "waves."

Initial conditions in Fig. 2 are defined by assuming that the time origin coincides with the beginning of the second cycle (point *S*). Thus density along x at $t = 0$ is K_2 for $0 \le x \le L_1$, K_1 for $L_1 \le x \le L_1 + L_2$ and variable between K_1 and K_2 for $L_1 + L_2 \le x \le L_1 + L_2 + L_3$. Actually initial conditions are defined by the real traffic conditions on the highway and therefore an infinite number of initial conditions exists. Since it is impossible to describe all possibilities Fig. 2 was drawn assuming that the system has reached a steady state. The analysis, however, for any arbitrary initial state is identical as demonstrated in the earlier work by Michalopoulos et al.[18] where derivation of the steady state (if it exists) and a detailed presentation of the traffic dynamics along the link downstream of line $B'B$ (Fig. 1) with or without the presence of a second signal can also be found. In this section only the analytical expressions for the characteristic lines and shock waves *KLM*, *PQR*, *NOV*, etc. are presented since they are necessary in the subsequent discussion. Thus the following equations apply for Fig. 2 assuming that $K_i^{(1)} = K_i^{(2)} = \cdots = K_i^{(n)} = K_i$ and $q_i^{(1)} = q_i^{(2)} = \cdots = q_i^{(n)} = q_i$, $i = 1, 2$.

$$\text{Slopes of characteristics } ZL \text{ and } SQ\text{: } h(K_1) = u_f(1 - 2K_1/K_j) \quad (5)$$

$$\text{Slopes of characteristics } SM \text{ and } JR\text{: } h(K_2) = u_f(1 - 2K_2/K_j) \quad (6)$$

Slope (speed) of shock wave KL and PQ:

$$h(K_1, K_2) = u_f(K_j - K_1 - K_2)/K_j. \tag{7}$$

From the above expressions it is possible to derive the following equations:

Characteristic ZL: $x = u_f(1 - 2K_1/K_j)(t + c)$ (8)

Characteristic SQ: $x = u_f(1 - 2K_1/K_j)t$ (9)

Characteristic SM: $x = u_f(1 - 2K_2/K_j)t$ (10)

Characteristic JR: $x = u_f(1 - 2K_2/K_j)(t - c)$ (11)

Shock wave PQ: $u_f(K_j - K_1 - K_2)(t - g_1)/K_j$. (12)

Point Q:

$$t_Q = \{(K_j - K_1 - K_2)g_1\}/(K_1 - K_2) \tag{13}$$

$$x_Q = \{(K_j - K_1 - K_2)(K_j - 2K_1)u_f g_1\}/\{K_j(K_1 - K_2)\}. \tag{14}$$

Shock wave QR:

$$x = h(K_2)t - [h(K_2) - h(K_1)]t_Q^{1/2}t^{1/2}. \tag{15}$$

Point R:

$$t_R = \{[h(K_2)c]^2(K_1 - K_2)\}/\{[h(K_2) - h(K_1)]^2(K_j - K_1 - K_2)g_1\} \tag{16}$$

$$x_R = \{(K_j - 2K_2)^3 u_f c^2\}/\{4K_j(K_1 - K_2)(K_j - K_1 - K_2)g_1\} - \{(K_j - 2K_2)u_f c/K_j\}. \tag{17}$$

Shock wave PQR beyond point R:

$$x = \epsilon t^{1/2}(t - c)^{1/2} \tag{18}$$

where:

$$\epsilon = x_R/\{t_R^{1/2}(t_R - c)^{1/2}\}. \tag{19}$$

Similarly, for shock wave KLM the following equations apply:

Shock wave KL:

$$x = \{u_f(K_j - K_1 - K_2)(t + c - g_1)\}/K_j. \tag{20}$$

Point L:

$$t_L = t_Q - c \tag{21}$$

$$x_L = x_Q \tag{22}$$

Shock wave LM:

$$x = h(K_2)(t + c) - [h(K_2) - h(K_1)](t_L + c)^{1/2}(t + c)^{1/2}. \tag{23}$$

Point M:

$$t_M = t_R - c \tag{24}$$

$$x_M = x_R \tag{25}$$

Shock wave KLM beyond point M:

$$x = \epsilon(t + c)^{1/2}t^{1/2} \tag{26}$$

It should be kept in mind that Eqs. 5 through 26 are also applicable (with only minor notational modifications) for unequal cycles and flow rates $q_1^{(n)}$, $q_2^{(n)}$. Furthermore, if $q_1 \simeq q_2$ points Q and R will occur at very long distances from line $B'B$ (Fig. 2). Therefore, if a downstream signal is present, points Q and R may not be realized. The existence of a downstream signal results into a large number of possible shock wave developments which are examined in the earlier work of Michalopoulos et al.[8] In the subsequent sections the basic modeling of Fig. 2 is employed first for deriving car paths and for studying in a macroscopic fashion the behavior of platoons as they move along the link. Afterward the case of a downstream signal is presented.

VEHICLE PATHS

FROM THE RESULTS presented to this point it is possible to derive analytical expressions for the trajectories (or paths) of cars as they travel along the link. These trajectories depend not only on the demands (q_i), the control policy and link characteristics (free flow speed, jam density, capacity) but also on their time of departure from line $B'B$ (Fig. 1). Thus, it is appropriate to differentiate between cars leaving during the green and red intervals. Before proceeding any further it should be clarified that, since the models employed throughout this analysis are macroscopic in nature, technically one cannot speak of individual cars but rather about a "mass" or group of cars which as it becomes smaller and smaller it can be practically assumed as a single car. Further, the term platoon used throughout this paper is loosely defined as any arbitrarily specified group of vehicles.

The trajectory of cars can be obtained from their speeds which at any time t and distance x (downstream of line $B'B$) depend on the density at this point. Again considering Greenshields model[6] speed is given by

$$dx/dt = u_f[1 - K(x, t)/K_j] \tag{27}$$

where $K(x, t)$ represents density at point x, t. From the modeling of the previous section it is seen that $K(x, t)$ can receive the value of K_1 or K_2 or it can lie in the interval $[K_2, K_1]$. If, however, x, t lies within the

downstream queue, $K(x, t)$ can also receive values in the range of $[K_j, K_m]$ where K_m represents the density at capacity. This case is treated in a subsequent section.

Integration of Eq. 27 yields the general equation of the car paths, i.e.,

$$x = \int_{t_0}^{t} u_f[1 - K(x, t)/K_j]\, dt \tag{28}$$

where $[t_0, t]$ is the time interval of interest. Equation 28 is useful for deriving the trajectories of cars departing at any arbitrary time from line $B'B$ (Fig. 1).

TRAJECTORIES OF CARS ENTERING IN GREEN

BASED ON THE previous discussion one can draw the path of any mass of cars entering the link. This is accomplished in Figure 3 which depicts the shock waves and the characteristic lines over three consecutive cycles as in Fig. 2. Line II in Fig. 3 represents the trajectory of a car (or more accurately, a mass of cars) entering the upstream end of the link during the green interval at time t_g $(0 \leq t_g \leq g_1)$. Segment AB of this trajectory is a straight line since between A and B density is constant and equals to K_1. Beyond B the car enters a zone of variable density and therefore its speed is time varying and its trajectory becomes more complex. From Eq. 27 it is seen that speed of the car from A to B (slope of line AB) is

$$dx/dt = u_f(1 - K_1/K_j). \tag{29}$$

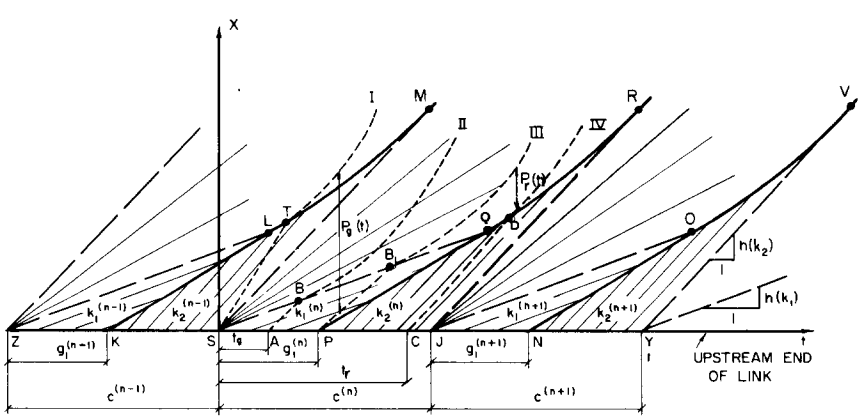

Fig. 3. Typical car paths.

Solution of this equation subject to the condition that $x = 0$ at $t = t_R$ yields the path AB as

$$x = u_f(1 - K_1/K_j)(t - t_R). \tag{30}$$

The coordinates of point B are given by the simultaneous solution of Eqs. 9 and 30, i.e.,

$$t_B = [(K_j - K_1)t_R]/K_1 \tag{31}$$

and

$$x_B = [u_f(K_j - K_1)(K_j - 2K_1)t_R]/(K_jK_1). \tag{32}$$

The car path beyond B is again derived by observing that the characteristic line passing through point x, t lying on the path is such that

$$x/t = u_f[1 - 2K(x, t)/K_j]. \tag{33}$$

The right hand side of the above expression equals to the slope of the tangent to the flow density curve at the point $q(x, t)$, $K(x, t)$; therefore the characteristic passing through x, t carries density $K(x, t)$. Solving Eq. 33 for $K(x, t)$ we obtain

$$K(x, t) = K_j[1 - x/u_f t]/2. \tag{34}$$

Substituting to Eq. 27 and making the necessary simplifications it follows that

$$dx/dt = [u_f + x/t]/2 \tag{35}$$

which is subject to the condition $x = x_B$ at $t = t_B$ and has the solution

$$x = u_f t - (u_f - x_B/t_B)(t_B t)^{1/2}. \tag{36}$$

Finally, substituting x_B and t_B from Eq. 31 and 32 one obtains the final form of the trajectory for the car path beyond point B (Fig. 2), i.e.,

$$x = u_f t - \{2u_f[K_1(K_j - K_1)t_R t]^{1/2}\}K_j. \tag{37}$$

Having developed the equations for any car leaving in green we can examine the path of the platoon head entering at the beginning of the effective green interval. Since the previous analysis is valid for any car leaving during green it is also valid for the platoon head entering the link at time $t_R = 0$ (Fig. 3). In such case points A and B coincide with S in Fig. 3 (since $t_R = 0$), and the platoon head enters an area of variable density immediately but only for an instant, i.e., at $t = 0$. In such case for $t_R = 0$ Eq. 37 yields:

$$x = u_f t \tag{38}$$

implying that the platoon head travels at free flow speed; this is true only if no cars are released during the previous red interval. Since, however,

non-zero flows during $r_1^{(n-1)}$ are unlikely, the platoon head follows the path shown by the dashed line I in Figure 3. Segment ST of this path is linear as the car enters a region of constant density $K_2^{(n-1)}$. As in the previous case the trajectory beyond point T is a more complex curve due to the time varying density downstream of T.

Returning to Figure 3 and by analogy with Eq. 30 it can be easily verified that line ST is given by

$$x = u_f[1 - K_2^{(n-1)}/K_j]t. \tag{39}$$

Simultaneous solution of Eqs. 23 and 39 yields the coordinates of point T, i.e.,

$$t_T = \{(2\alpha\beta c + t_L + c) - [(2\alpha\beta c + t_L + c)^2 - 4\beta^2(c^2\alpha^2 - c^2 - ct_L)]^{1/2}\}/(2\beta^2) \tag{40}$$

where

$$\alpha = [K_j - 2K_2^{(n-1)}]/\{2[K_1^{(n-1)} - K_2^{(n-1)}]\} \tag{41}$$

and

$$\beta = K_2^{(n-1)}/\{2[K_1^{(n-1)} - K_2^{(n-1)}]\}. \tag{42}$$

Finally

$$x_T = \{u_f[K_j - K_2^{(n-1)}]t_T\}/K_j. \tag{43}$$

Similarly noting that the characteristics beyond T emanate from the beginning of the previous effective green interval (point Z), i.e., at $t = t_z = -c$, one can derive the equation of line I after time T which may be written as

$$x = u_f(t + c) - [u_f - x_T/(t_T + c)][(t_T + c)(t + c)]^{1/2}. \tag{44}$$

It should be evident that point T (Fig. 3) can occur before L; in such case the path of the car leaving at the beginning of green is shown by line STV_1 in Fig. 4. The change in speed after point T is due to the higher density $K_1^{(n-1)}$ which is maintained up to point V_1. Thus Eq. 39 is still valid for segment ST but the coordinates of point T are now given by

$$t_T = \{[K_j - K_1^{(n-1)} - K_2^{(n-1)}][c - g_1^{(n-1)}]\}/K_1^{(n-1)} \tag{45}$$

$$x_T = \{u_f[K_j - K_2^{(n-1)}]t_T\}/K_j. \tag{46}$$

Furthermore, line TV_1 can be expressed as

$$x = x_T + u_f(1 - K_1^{(n-1)}/K_j)(t - t_T). \tag{47}$$

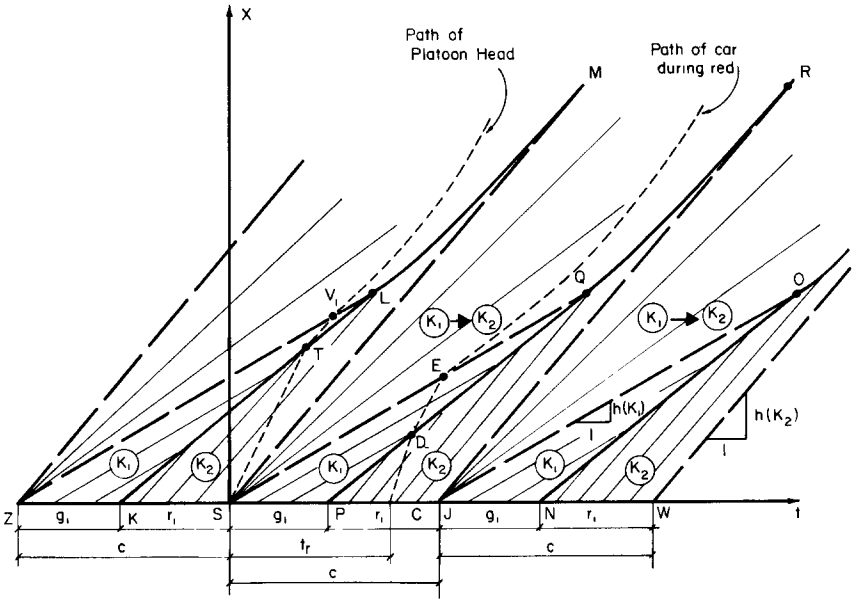

Fig. 4. Alternative paths for platoon head and tail.

And the coordinates of point V_1 are

$$t_{V1} = \{[(K_j - 2K_1^{(n-1)})c] + [(K_j - K_1^{(n-1)})t_T]\}/K_1^{(n-1)} \quad (48)$$

$$x_{V1} = \{u_f(K_j - K_1^{(n-1)})(K_j - 2K_1^{(n-1)})(t_T + c)\}/(K_j K_1^{(n-1)}). \quad (49)$$

Finally the car path beyond V_1 is given from

$$x = u_f(t + c) - [u_f - x_{V1}/(t_{V1} + c)](t_{V1} + c)^{1/2}(t + c)^{1/2}. \quad (50)$$

One can of course determine the proper path between the ones shown in Figs. 3 and 4 by comparing t_L, given from Eq. 21, with t_T from Eq. 45. In fact from these equations it can be shown that the path of Fig. 4 will be followed if

$$g_1^{(n)}/c \geq \{[K_j - K_1^{(n-1)}][K_1^{(n-1)} - K_2^{(n-1)}]\}/$$
$$\{[K_j - K_1^{(n-1)} - K_2^{(n-1)}][2K_1^{(n-1)} - K_2^{(n-1)}]\}. \quad (51)$$

The path of any car entering the link in green can be determined from the equations presented to this point. Therefore, one can easily determine the trajectories of the head and tail for any group of vehicles which in a broad sense can be considered as a platoon. For example, such a platoon is the group of cars entering the link during the entire green interval; its head includes the mass of the first car(s) entering at the beginning of green and its tail consists of the last car(s) entering at the end of the

green interval. The trajectory of the tail is shown by the dashed line *III* in Fig. 3. Since the positions of both platoon head and tail at any time are given from Eqs. 30 through 51, the distance between them (defined here as platoon length, P_g) can be computed and its evolution in time can be studied.

TRAJECTORIES OF CARS ENTERING IN RED

THE TRAJECTORIES of cars entering the link during the red interval can be derived in a similar fashion. The two possible paths are shown by the dashed lines *IV* and *CDE* in Figs. 3 and 4, respectively. In summary, the following equations apply for the path *CDE* in Fig. 4.

Path *CD*:

$$x = \{u_f(K_j - K_2)(t - t_r)\}/K_j. \tag{52}$$

Point *D*:

$$t_D = \{(K_j - K_2)t_r - (K_j - K_1 - K_2)g_1\}/K_1 \tag{53}$$

$$x_D = \{u_f(K_j - K_2)(K_j - K_1 - K_2)(t_r - g_1)\}/(K_jK_1). \tag{54}$$

Path *DE*:

$$x = x_D + [u_f(K_j - K_1)(t - t_D)\}/K_j. \tag{55}$$

Point *E*:

$$t_E = \{(K_j - K_1)t_D - K_jx_D/u_f\}/K_1 \tag{56}$$

$$x_E = \{u_f(K_j - 2K_1)t_E\}/K_j. \tag{57}$$

Path Beyond *E*:

$$x = u_ft - (u_f - x_E/t_E)t_E^{1/2}t^{1/2}. \tag{58}$$

If line *CD* intersects shock wave *PQ* after $t = t_Q$ then the path of Fig. 4 is changed to that shown by line *IV* in Fig. 3 in which

$$t_D = \{[(K_1 - K_2)^2t_Q + K_2(K_j - K_2)t_r]^{1/2} - (K_1 - K_2)t_Q^{1/2}\}^2/K_2^2 \tag{59}$$

$$\mathrm{x}_D = [\mathrm{u}_f(\mathrm{K}_j - \mathrm{K}_2)\mathrm{t}_D - \mathrm{t}_r)]/\mathrm{K}_j \tag{60}$$

and the position of the car beyond point *D* is

$$x = u_ft - (u_f - x_D/t_D)t_D^{1/2}t^{1/2}. \tag{61}$$

As before, one can easily determine whether the path of Fig. 3 or Fig. 4 will be followed by comparing t_D from Eq. 53 to t_Q given by Eq. 13; from

these two expressions it can be verified that the path of Fig. 4 will be followed if

$$t_r/g_1 \leq \{(2K_1 - K_2)(K_j - K_1 - K_2)\}/\{(K_1 - K_2)(K_j - K_2)\}. \quad (62)$$

Based on the above expressions the behavior of platoons entering the link during the red interval can also be studied. For example, if platoon head is defined as the first car(s) entering at the beginning of red, its path is shown by line *III* in Fig. 3 (which at the same time represents the tail of a platoon in green) and is defined by the following expressions.

Path PB_1:

$$x = \{u_f(K_j - K_1)(t - g_1)\}/K_j \quad (63)$$

Point B_1:

$$t_{B1} = \{(K_j - K_1)g_1\}/K_1 \quad (64)$$

$$x_{B1} = \{u_f(K_j - K_1)(K_j - 2K_1)g_1\}/(K_jK_1) \quad (65)$$

Path Beyond B_1:

$$x = u_f t - (u_f - x_{B1}/t_{B1})t_{B1}^{1/2}t^{1/2}. \quad (66)$$

For any arbitrarily chosen platoon tail the sets of Eqs. 52 through 58 and 52, 59, 60, 61 apply. Unless otherwise specified in the subsequent discussion, when platoons entering in red are studied the entire group of cars entering the link during red will be considered, i.e., platoon tail enters at the end of red.

PLATOON LENGTHS

AS MENTIONED earlier, having developed analytical expressions for the paths it is possible to consider the distance between the leading and trailing end of any arbitrarily selected group of vehicles entering the link and study its evolution in time and space. In this section the lengths of the platoons entering the link in green are examined first and subsequently the results are extended for the red intervals.

In order to simplify presentation of the results consider initially the path of the first car entering the link in green when no cars are released in the previous red interval. This path is given by Eq. 38 which suggests that the head moves with free flow speed; since the platoon tail is expressed by Eqs. 30 and 36, platoon length before or after point B (Fig.

3) is given from

$$P_g(t) = [(u_f K_1 t)/K_j] + [u_f(K_j - K_1)t_g]/K_j,\ t_g \le t < t_B \quad (67)$$

$$P_g(t) = (u_f - x_B/t_B){t_B}^{1/2}t^{1/2},\ t \ge t_B. \quad (68)$$

Inspection of the above two expressions clearly suggests that platoon length expands with time, i.e., platoon disperses. This of course is not unexpected since platoon tail moves with speed lower than u_f. Let us now examine the most realistic case in which cars are actually released in the previous cycle. From the discussion of the previous sections it should be evident that due to the many segments of the head and tail paths one should examine platoon lengths for a number of successive time intervals resulting by inspection of Figs. 3 and 4. For the purpose of illustrating the analysis assume that $t_T > t_L$ so that Fig. 3 and Eqs. 39 through 44 apply for the path of the head. Further consider the case in which t_g is such that $t_B < t_T$ and suppose that one is interested to examine platoon length developments between points B and T, i.e., during the interval $t_g < t_B \le t < t_T$. In this case the expressions for the head and tail paths are given by Eqs. 36 and 39, respectively, and therefore platoon length is

$$P_g(t) = u_f\{[1 - x_B/(u_f t_B)]{t_B}^{1/2}t^{1/2} - ({K_2}^{(n-1)}t)/K_j\}.$$

From this expression it is not evident whether platoon length increases or decreases with time. However, it is possible to identify the time interval of expansion by setting

$$dP_g(t)/dt = u_f\{[1 - x_B/(u_f t_B)]{t_B}^{1/2}/(2t^{1/2}) - {K_2}^{(n-1)}/K_j\} \ge 0,$$

which is satisfied for

$$t \le K_j^2[1 - x_B/(u_f t_B)]^2 t_B/[4({K_2}^{(n-1)})^2] = t_e.$$

Thus for $t_B \le t \le t_e$ platoon expands and for $t_e < t \le t_T$ platoon contracts.

Similar analysis can be performed also for the case $t_T < t_B$ (which actually corresponds to Fig. 3 and for all time intervals. Referring to Fig. 3 it can be seen that for a more systematic analysis one should start by first studying the interval $t_g \le t \le t_T < t_B$, then the case in which $t_B < t_T$. Following this interval $t_g < t_T < t < t_B$ can be examined and so on. Due to the lengthy derivations the results for each time interval and possible occurrence of points L, T, B, and V_1 in Figs. 3 and 4 are systematically summarized in Tables I and II, respectively. The second column of each table denotes the time interval of interest which in turn depends on t_g and the time of occurrence of points T, B, and V_1. The third column refers to the equation of the platoon head and tail employed for deriving platoon lengths presented in column 4. Finally the last column shows the upper bound of expansion or compression within the time interval of

TABLE I

Summary of Platoon Length Properties During Green: $t_T > t_L$ (Fig. 3)

1	2	3		4	5
Case	Time t	Eq for Position of Head x_h	Eq for Position of Tail x_t	Platoon Length $P_g(t) = x_h - x_t$	Remarks
a	$t_g \le t < t_T < t_B$	(39)	(30)	$\{u_f[(K_1 - K_2^{(n-1)})t + (K_j + K_1)t_g]\}/K_j$	Expansion only
b	$t_g \le t < t_B < t_T$	(39)	(30)	As in Case a	Expansion only
c	$t_g < t_T \le t < t_B$	(44)	(30)	$u_f\{c - [1 - x_T/(u_f(t_T + c))](t_T + c)^{1/2}(t + c)^{1/2} + [K_1 t + (K_j - K_1)t_g]/K_j\}$	Contraction for $t \le K_j^2\{[1 - x_T/(u_f(t_T + c))]^2(t_T + c)/[4K_1^2]\} - c$
d	$t_g < t_T < t_B \le t$	(44)	(36)	$u_f\{c - [1 - x_T/(u_f(t_T + c))](t_T + c)^{1/2}(t + c)^{1/2} + [1 - x_B/(u_f t_B)]t_B^{1/2}t^{1/2}\}$	Expansion for $t \le c\{[[1 - x_T/(u_f(t_T + c))]^2(t_T + c)]/[[1 - x_B/(u_f t_B)]^2 t_B] - 1\}^{-1}$
e	$t_g < t_B < t_T \le t$	(44)	(36)	As in Case d	As in Case d
f	$t_g < t_B \le t < t_T$	(39)	(36)	$u_f\{[1 - x_B/(u_f t_B)]t_B^{1/2}t^{1/2} - [K_2^{(n-1)}t]/K_j\}$	Expansion for $t \le K_j^2\{[1 - x_B/(u_f t_B)]^2 t_B\}/[4(K_2^{(n-1)})^2]$

TABLE II

Summary of Platoon Length Properties During Green: $t_T < t_L$ (Fig. 4)

1	2	3		4	5
Case	Time t	Eq for Position of Head x_h	Eq for Position of Tail x_t	Platoon Length $P_n(t) = x_h - x_t$	Remarks
a	$t_g \le t < t_B < t_T < t_{V1}$	(39)	(30)	$\{u_f[(K_1 - K_2^{(n-1)})t + (K_j - K_1)t_g]\}/K_j$	Expansion only
b	$t_g \le t < t_T < t_B < t_{V1}$	(39)	(30)	As in Case a	Expansion only
c	$t_g \le t < t_T < t_{V1} < t_B$	(39)	(30)	As in Case a	Expansion only
d	$t_g < t_B \le t < t_T < t_{V1}$	(39)	(36)	$u_f\{[1 - x_B/(u_f t_B)]t_B^{1/2}t^{1/2} - K_2^{(n-1)}t/K_j\}$	Expansion for $t \le K_j^2\{[1 - x_B/(u_f t_B)]^2 t_B\}/[4(K_2^{(n-1)})^2]$
e	$t_g < t_B < t_T \le t < t_{V1}$	(47)	(36)	$x_T + u_f\{(K_j - K_1)t_T/K_j - K_1 t/K_j + [1 - x_B/(u_f t_B)]t_B^{1/2}t^{1/2}\}$	Expansion for $t \le K_j^2\{[1 - x_B/(u_f t_B)]^2 t_B\}/[4K_1^2]$
f	$t_g < t_T < t_B \le t < t_{V1}$	(47)	(36)	As in Case e	As in Case e
g	$t_g < t_B < t_T < t_{V1} \le t$	(50)	(36)	$u_f\{c + [1 - x_B/(u_f t_B)]t_B^{1/2}t^{1/2} - [1 - x_{V1}/(u_f(t_{V1} + c))](t_{V1} + c)^{1/2}(t + c)^{1/2}\}$	Expansion for $t \le c\{[[1 - x_{V1}/(u_f(t_{V1} + c))]^2(t_{V1} + c)]/[[1 - x_B/(u_f t_B)]^2 t_B] - 1\}^{-1}$
h	$t_g < t_T < t_B < t_{V1} \le t$	(50)	(36)	As in Case g	As in Case g
i	$t_g < t_T < t_{V1} < t_B \le t$	(50)	(36)	As in Case g	As in Case g
j	$t_g < t_T \le t < t_B < t_{V1}$	(47)	(30)	$x_T - \{u_f[(K_j - K_1^{(n-1)})t_T - (K_j - K_1^{(n)})t_g - (K_1^{(n)} - K_1^{(n-1)})t]\}/K_j$	Expansion if $K_1^{(n)} > K_1^{(n-1)}$ Constant if $K_1^{(n)} = K_1^{(n-1)}$ Contraction if $K_1^{(n)} < K_1^{(n-1)}$
k	$t_g < t_T \le t < t_{V1} < t_B$	(47)	(30)	As in Case j	As in Case j
l	$t_g < t_T < t_{V1} \le t < t_B$	(50)	(30)	$u_f\{c - [1 - x_{V1}/(u_f(t_{V1} + c))](t_{V1} + c)^{1/2}(t + c)^{1/2} + K_1 t/K_j + (K_j - K_1)t_g/K_j\}$	Contraction for $t \le K_j^2\{[1 - x_{V1}/(u_f(t_{V1} + c))]^2(t_{V1} + c)\}/[4K_1^2]$

column 2. Inspection of Tables I and II and the discussion to this point leads to the conclusion that platoon compression is possible even for platoons released in green despite the absence of a downstream bottleneck. This should of course be attributed to the traffic released in earlier cycles which causes the platoon head to slow down as it enters an area of higher density.

Following similar guidelines an analysis for the platoons entering the link during red can also be performed. As another example consider Fig. 3 in which the path of a car released in red at $t = t_r$ is such that $t_D > t_Q$. If platoon head enters at the beginning of red and $t_{B1} < t_D$ then in the interval $t_r < t_{B1} \leq t < t_D$ Eqs. 66 and 52 apply and platoon length $P_r(t)$ is

$$P_r(t) = \{u_f K_2 t/K_j - [1 - x_{B1}/(u_f t_{B1})]t_{B1}^{1/2} t^{1/2} + (K_j - K_2)t_r/K_j\}.$$

For platoon compression $dP_r(t)/dt < 0$ or

$$dP_r(t)/dt = u_f\{K_2/K_j - [1 - x_{B1}/(u_f t_{B1})]t_{B1}^{1/2}/(2t^{1/2})\} \leq 0.$$

This inequality is satisfied for

$$t \leq K_j^2\{[1 - x_{B1}/(u_f t_{B1})]^2 t_{B1}\}/(4K_2^2) = t_c$$

therefore in the interval $t_r < t_{B1} < t \leq t_c$ platoon length decreases (compression) and during $t_c < t < t_D$ it increases (dispersion). Again due to space limitations the dynamics of platoons entering on red are summarized in Tables III and IV which include all time intervals for the two possible paths of the platoon tail depicted in Figs. 3 and 4. These tables are similar in format with the previous two. It is reminded at this point that the tables were completed by observing that the path of the platoon head is given by Eqs. 63 and 66. Inspection of Tables III and IV suggests that both compression and dispersion is possible for the platoons entering on red. The former should of course be expected as platoons entering in red meet with traffic of higher density released during the green interval. However, expansion was not intuitively evident before this analysis and it is of course explained by the increased speed of the platoon head as it enters regions of lower density (i.e., beyond B_1 in Fig. 3) or the decreased velocity of the platoon tail as it enters areas of higher density formed by the traffic released earlier in green. Finally it is reminded that the results presented to this point do not take into consideration the effects of a downstream signal, i.e., no signal is assumed at the downstream end of the link. The effects of a downstream signal are discussed in a subsequent section.

FLOW RATE CONSIDERATIONS

IN ADDITION to platoon lengths, flow rates at any point downstream of the traffic signal can be expressed as functions of time for demonstrating

TABLE III

Summary of Platoon Length Properties During Red: $t_D > t_Q$ (Fig. 3)

1	2	3		4	5
Case	Time t	Eq for Position of Head x_h	Eq for Position of Tail x_t	Platoon Length $P_r(t)$	Remarks
a	$t_r \le t < t_{B1} < t_D$	(63)	(52)	$\{u_f[(K_j - K_2)t_r - (K_j - K_1)g_1 - (K_1 - K_2)t]\}/K_j$	Contraction only
b	$t_r \le t < t_D < t_{B1}$	(63)	(52)	As in Case a	Contraction only
c	$t_r < t_{B1} \le t < t_D$	(66)	(52)	$u_f\{K_2t/K_j - [1 - x_{B1}/(u_ft_{B1})]t_{B1}^{1/2}t^{1/2} + (K_j - K_2)t_r/K_j\}$	Contraction for $t \le K_j^2\{[1 - x_{B1}/(u_ft_{B1})]^2t_{B1}\}/[4K_2^2]$
d	$t_r < t_{B1} < t_D \le t$	(66)	(61)	$u_f\{[1 - x_D/(u_ft_D)]t_D^{1/2}t^{1/2} - [1 - x_{B1}/(u_ft_{B1})]t_{B1}^{1/2}t^{1/2}\}$	Expansion only

TABLE IV

Summary of Platoon Length Properties During Red: $t_D < t_Q$ (Fig. 4)

1	2	3		4	5
Case	Time t	Eq for Position of Head x_h	Eq for Position of Tail x_t	Platoon Length $P_r(t)$	Remarks
a	$t_r \le t < t_{B1} < t_D < t_E$	(63)	(52)	$\{u_f[(K_j - K_2)t_r - (K_j - K_1)g_1 - (K_1 - K_2)t]\}/K_j$	Contraction only
b	$t_r \le t < t_D < t_{B1} < t_E$	(63)	(52)	As in Case a	Contraction only
c	$t_r < t_{B1} \le t < t_D < t_E$	(66)	(52)	$u_f\{K_2t/K_j - [1 - x_{B1}/(u_ft_{B1})]t_{B1}^{1/2}t^{1/2} + (K_j - K_2)t_r/K_j\}$	Contraction for $t \le K_j^2\{[1 - x_{B1}/(u_ft_{B1})]^2t_{B1}\}/[4K_2^2]$
d	$t_r < t_{B1} < t_D < t_E \le t$	(66)	(58)	$u_f\{[1 - x_E/(u_ft_E)]t_E^{1/2}t^{1/2} - [1 - x_{B1}/(u_ft_{B1})]t_{B1}^{1/2}t^{1/2}$	Expansion only
e	$t_r < t_D < t_{B1} < t_E \le t$	(66)	(58)	As in Case d	As in Case d
f	$t_r < t_{B1} < t_D \le t < t_E$	(66)	(55)	$u_f\{K_1t/K_j - [1 - x_{B1}/(u_ft_{B1})]t_{B1}^{1/2}t^{1/2} + (K_j - K_1)t_D/K_j\} - x_D$	Contraction for $t \le K_j^2\{[1 - x_{B1}/(u_ft_{B1})]^2t_{B1}\}/[4K_1^2]$
g	$t_r < t_D < t_{B1} \le t < t_E$	(66)	(55)	As in Case f	As in Case f
h	$t_r < t_D \le t < t_{B1} < t_E$	(63)	(55)	$u_f(K_j - K_1)(t_D - g_1)/K_j - x_D$	Constant always

platoon compression as well as diffusion. This is accomplished by inspection of Fig. 5 which shows shock wave developments over three consecutive cycles as in Fig. 2. Again distance is measured from the upstream end of the link (line $B'B$ in Fig. 1) and point S is taken as the time origin. Shock waves KLM and PQR are identical to those of Fig. 2, while $Z_4Z_6Z_8$ and Z_5Z_7 begin two and three cycles before S. These lines and the characteristics Z_3Z_6, Z_2L, SM, SQ and JR divide the time space domain into zones of constant and variable densities which are in the range $[K_2, K_1]$. From the assumed speed-density relationship, flow rate at any point (x, t) is given from

$$q(x, t) = u_f\{K(x, t) - [K(x, t)]^2/K_j\}. \tag{68a}$$

From Fig. 5 it is seen that flow rate at a fixed point along the link does not only depend on time but is also a function of the point location relative to the points Q and R. There are three possibilities a) $x \leq x_Q$, b) $x_Q < x \leq x_R$, and c) $x_R < x$; lines S_1J_1, S_2J_2, and S_3J_3 were drawn for examining each case.

Considering the first-possibility for distance $x_1 \leq x_Q$ it is observed that density between points S_1 and S_1' varies in the range $[K_2, K_1]$ from S_1' to J_1' density equals to K_1 and from J_1' to J_1 it is K_2. The slope of the characteristics passing through S_1S_1' is

$$h[K(x_1, t)] = u_f[1 - 2K(x_1, t)/K_j] = x_1/t \tag{68b}$$

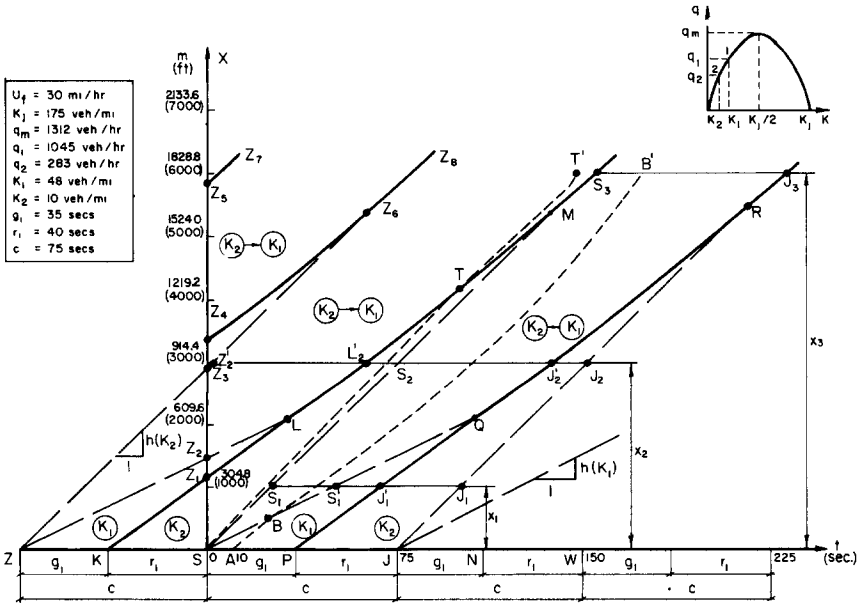

Fig. 5. Flow rate derivation and numerical example.

therefore,

$$K(x_1, t) = \{K_J[1 - x_1/(u_f t)]\}/2 \tag{69}$$

and substituting to Eq. 68a

$$q(x_1, t) = K_J[u_f - x_1^2/(u_f t^2)]/4 \tag{70}$$

for $t_{S1} \leq t \leq t_{S1'}$; t_{S1} and $t_{S1'}$ are given from

$$t_{S1} = x_1/h(K_2) \tag{71}$$

$$t_{S1'} = x_1/h(K_1). \tag{72}$$

Since between points S_1' and J_1' density is K_1

$$q(x_1, t) = u_f[K_1 - K_1^2/K_J],\ t_{S1'} \leq t \leq t_{J1'} \tag{73}$$

where

$$t_{J1'} = [x_1/h(K_1, K_2)] + g_1 \tag{74}$$

and $h(K_1, K_2)$ is given from Eq. 7. Finally, flow rate from J_1' to J_1

$$q(x_1, t) = u_f[K_2 - K_2^2/K_J], \qquad t_{J1'} \leq t \leq t_{J1} \tag{75}$$

where

$$t_{J1} = [x_1/h(K_2)] + c. \tag{76}$$

It should be noted that Eq. 75 also gives the flow rate in the interval $[0, t_{S1}]$ in which density equals to $K_2^{(n-1)}$; similarly Eq. 70 can be used for the time interval immediately after point J_1 due to the repetitive pattern of the traffic flows. Stated otherwise, Eqs. 70, 73 and 75 allow estimation of the flow rates at distance x_1 due to the traffic released at the present cycle. The same expressions, however, are valid for the traffic released in any cycle such as the next, or the previous.

Following similar logic the flow rates for the remaining two cases, i.e., $x_Q < x_2 \leq x_R$ and $x_R < x_3$, were derived. In summary, the following expressions hold along line S_2J_2. For $t_{S2} < t < t_{J2'}$:

$$q(x_2, t) = \{K_J[u_f - x_2^2/(u_f t^2)]\}/4 \tag{77}$$

where

$$t_{S2} = x_2/h(K_2) \tag{78}$$

$$t_{J2'} = \{[h(K_2) - h(K_1)]t_Q^{1/2} + [(h(K_2) - h(K_1))^2 t_Q + 4x_2 h(K_2)]^{1/2}\}^2/\{4[h(K_2)]^2\}. \tag{79}$$

For $t_{J2'} \leq t \leq t_{J2}$

$$q(x_2, t) = u_f[K_2 - K_2^2/K_j] \tag{80}$$

where

$$t_{J2} = [x_2/h(K_2)] + c. \tag{81}$$

It is noted that flow rate in the interval $[0, t_{Z2'}]$ is given from Eq. 80 but K_2 should be replaced with $K_2^{(n-2)}$ and in the interval $[t_{Z2}, t_{L2'}]$ from Eq. 77 by setting $t = t + c$. Finally for $t_{L2'} \leq t \leq t_{S2}$ q is given from Eq. 80 by setting $K_2 = K_2^{(n-1)}$; $t_{Z2'}$ and $t_{L2'}$ are obtained in a manner similar to t_{S2} and $t_{J2'}$, respectively.

The last case $x_R < x_3$ is characterized by variable density along the entire range $[t_{S3}, t_{J3}]$ in which

$$q(x_3, t) = [K_j\{1 - x_3^2/(u_f t^2)\}]/4 \tag{82}$$

where

$$t_{S3} = x_3/h(K_2) \tag{83}$$

$$t_{J3} = \{c + [c^2 + 4x_3^2/\epsilon^2]^{1/2}\}/2. \tag{84}$$

Flow rate before t_{S3} or after t_{J3} are obtained similarly by shifting backward or forward in time.

Numerical examples presented in a subsequent section demonstrate the use of the results presented to this point. Before this is accomplished, however, it is appropriate to examine the effects of a downstream signal. This is the subject of the following section.

THE CASE OF A DOWNSTREAM SIGNAL

IF A SIGNAL is present at the downstream end of the link the analysis of the previous section is still valid up to the point at which the cars meet the tail end of the queue. The trajectory of the queue tail at the downstream signal can be found according to the methodology proposed by Michalopoulos et al.[8] and is a function of the control policy (cycle, green intervals at both signals, offset) the link characteristics (capacity, u_f, K_j) and the demands. Due to the many combinations of these variables a large number of patterns for the trajectory of the queue tail are possible. Figure 6 presents one possibility for two consecutive saturated cycles. Line $ACDA'C'D'A''$ is the trajectory of the queue tail which can be derived numerically or analytically as suggested by Michalopoulos et al.[8] In Figure 6 lines AB and $A'B'$ represent the initial queue length (in which density corresponds to jam conditions) and lines GD and $G'D'$ are shock waves generated at the beginning of the red intervals. The characteristic lines emanating from the boundaries AB, $A'B'$ and the stop

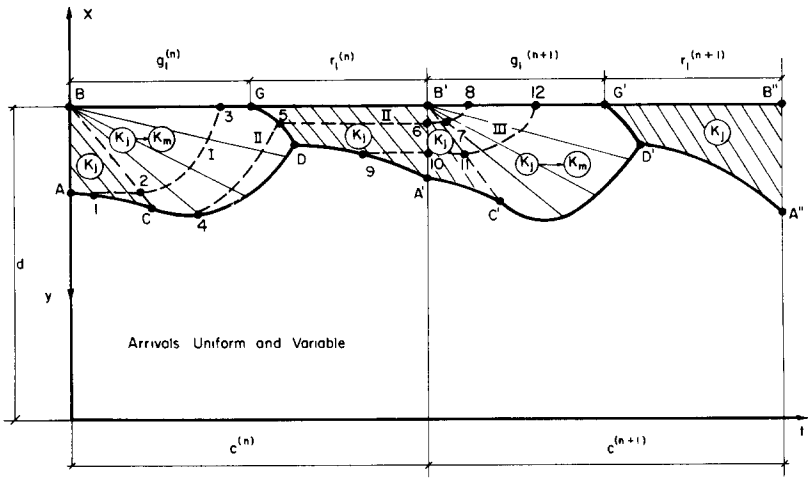

Fig. 6. Queue length and car paths at the downstream end of the link.

line ($x = d$) suggest that within the queue length $y(t)$ density conditions range from jam to capacity. This in fact holds true irrespectively of the exact shape of the trajectory of the queue tail and therefore it is possible to develop general car path equations after a car enters the queue. Returning to Figure 6 it is observed that, within the zones of parallel characteristic lines, K equals to K_j while zones with fanning characteristics suggest that density varies from K_j to K_m (capacity).

Lines *I*, *II*, and *III* in Figure 6 represent the three general car path patterns after the cars enter the downstream queue. In the first path the car joins the queue shortly after the commencement of green at point 1 while at the tail end density still equals to K_j. Therefore, the car is forced to stop (i.e., its speed is zero) until point 2 when density conditions in front of it improve. Thus at $t = t_2$ the car begins to move again and at $t = t_3$ it crosses the stop line. If the coordinates x_1, t_1 are known the car path can be derived. Segment 1-2 is of course given from $x = x_1$; its intersection with line $AC(x = d - u_f t)$ yields

$$t_2 = (d - x_1)/u_f \tag{85}$$

$$x_2 = x_1 = d - u_f t_2 \tag{86}$$

for the segment beyond point 2

$$dx/dt = u_f\{1 - K(x, t)/K_j\}; \tag{87}$$

however,

$$h[K(x, t)] = -u_f[1 - 2K(x, t)/K_j] = (d - x)/t. \tag{88}$$

Solving Eq. 88 for $K(x, t)$ one obtains,

$$K(x, t) = K_j[1 + (d - x)/(u_f t)]/2. \tag{89}$$

Substituting $K(x, t)$ to Eq. 87

$$dx/dt = [u_f - (d - x)/t]/2. \tag{90}$$

Solution of Eq. 90, subject to the condition $x = x_2 = x_1$ at $t = t_2$, yields the car path 2-3

$$x = d + u_f t - [u_f + (d - x_2)/t_2](t_2 t)^{1/2} \tag{91}$$

from which

$$t_3 = [1 + (d - x_2)/(u_f t_2)]^2 t_2 \tag{92}$$

since

$$x_3 = d. \tag{93}$$

If the car happens to reach the tail end of the queue at $t = t_4$ such that $t_C < t_4 < g$ it will not stop and its trajectory is represented by line *II* (Fig. 6). It should be noted that the possibility that the car clears the intersection during green cannot be excluded; in such case point 5 falls on the stop line. Thus Fig. 6 actually depicts the case in which the car arrives late and is released in the next cycle. In summary, the following expressions are valid for path *II*

Segment 4-5:

$$x = d + u_f t - [u_f + (d - x_4)/t_4](t_4 t)^{1/2} \tag{94}$$

$$t_5 = \{[1 - (d - x_4)/(u_f t_4)]t_4^{1/2} + [g_1^{(n)}]^{1/2}\}^2/4 \tag{95}$$

$$x_5 = d - u_f t_5 + u_f\{g_1^{(n)}\}^{1/2} t_5^{1/2} \tag{96}$$

Segment 5-6:

$$x = x_5 \tag{97}$$

$$t_6 = c \tag{98}$$

$$x_6 = x_5 \tag{99}$$

Segment 6-7:

$$x = x_6 \tag{100}$$

$$t_7 = (d - x_6)/u_f + c \tag{101}$$

$$x_7 = x_6 \tag{102}$$

Segment 7–8:

$$x = d + u_f(t - c) - [u_f - (d - x_7)/(t_7 - c)](t_7 - c)^{1/2}(t - c)^{1/2} \quad (103)$$

$$t_8 = [1 - (d - x_7)/(u_f(t_7 - c))]^2(t_7 - c) + c \quad (104)$$

$$x_8 = d. \quad (105)$$

As pointed out earlier, the car could depart in the same cycle it arrives so that point 5 falls on the stop line, i.e., $x_5 = d$; in such case by putting $x = d$ in Eq. 94 and solving it for t,

$$t_5 = [1 + (d - x_4)/(u_f t_4)]^2 t_4. \quad (105a)$$

This situation arises only when t_5 from Eq. 105a is less than g_1. Therefore, putting $t_5 < g_1$ it can be verified that departure in green occurs if

$$t_4 \leq \{g_1^{1/2} + [g_1 - 4(d - x_4)/u_f]^{1/2}\}^2/4. \quad (105b)$$

Line *III* in Fig. 6 represents the path of a car arriving in red at $t = t_9$ and clearing the intersection during the next cycle at $t = t_{12}$. For this case it can easily be verified that

For Segment 9–10:

$$x = x_9 \quad (106)$$

$$t_{10} = c \quad (107)$$

$$x_{10} = x_9 \quad (108)$$

for Segment 10–11:

$$x = x_{10} \quad (109)$$

$$t_{11} = [1 + (d - x_9)/(u_f(t_9 - c))]^2(t_9 - c) + c \quad (110)$$

$$x_{11} = x_{10} \quad (111)$$

for Segment 11–12:

$$x = d + u_f(t - c) - [u_f - (d - x_{11})/(t_{11} - c)](t_{11} - c)^{1/2}(t - c)^{1/2}. \quad (112)$$

It is, however, possible that the car arriving on red does not clear the intersection in the next cycle. In such case point 12 falls on line $G'D'$ and a path similar to segment 5–6–7–8 is followed. The latest time (t_9) a car should arrive on red so that it clears during the next cycle can easily be found by letting $x_{12} = d$, $t_{12} = t$ in Eq. 112 solving for t_{12} and setting $t_{12} \leq g^{(n+1)} + c$.

It should be remembered that Figure 6 does not include undersaturated cycles. Extension for such cycles is in fact straight forward. For example for early queue arrivals ($t_1 < t_C$) path *I* remains unchanged. Path *II* is

also applicable for any arrival in green after t_C the only difference being that point 5 falls on the stop line its time coordinate is as given by Eq. 105a and all cars arriving on green depart before the commencement of red. Finally, path *III* is not affected i.e., it is the same for both saturated and undersaturated cycles.

NUMERICAL RESULTS

THE FOLLOWING EXAMPLE illustrates the applicability of the results presented to this point and clearly demonstrates platoon compression by examining platoon lengths, car paths and flow rates at various distances along the highway. Assume that the link in question is very long (i.e., no downstream signal is present) and has the following characteristics

Free flow speed: $u_f = 48$ km/h (30 mi/h)
Jam density: $K_j = 109.4$ veh/km (175 veh/mi)
Capacity of link: $q_m = 1312$ veh/h
Upstream effective green: $g_1 = 35$ s
Upstream effective red: $r_1 = 40$ s
Cycle length: $c = 75$ s
Flow rates at upstream end of link:
During green: $q_1 = q_1^{(1)} = q_1^{(2)} = \cdots = q_1^{(n)} = 1045$ veh/h $\rightarrow K_1 = 30$ veh/km (48 veh/mi)
During red: $q_2 = q_2^{(1)} = q_2^{(2)} = \cdots = q_2^{(n)} = 283$ veh/h $\rightarrow K_2 = 6.3$ veh/km (10 veh/mi)

From Eqs. 5, 6 and 7 it can be verified that $h(K_1) = 6.1$ m/s (19.95 ft/s), $h(K_2) = 11.9$ m/s (39 ft/s), and $h(K_1, K_2) = 9$ m/s (29.5 ft/s); further, from Eqs. 13, 14, 16, 17 and 19 $t_Q = 108$ s, $x_Q = 625.6$ m (2141 ft), $t_R = 217$ s, $x_R = 1688$ m (5538 ft) and $\epsilon = 9.6$ m/s (31.55 ft/s). From these results and Eqs. 21, 22, 24, and 25 it can be seen that $t_L = 33$ s, $x_L = 625.6$ m (2141 ft), $t_M = 142$ s, and $x_M = 1688$ m (5538 ft). Referring to Figure 5 it is observed that from this information shock waves *KLM*, *PQR* and the characteristics *SM* and *JR* can be plotted. The remaining points in Figure 5 which are necessary in the following discussion can be found by using the results of the previous sections. Thus from Eq. 20 and noting that $t_K = -r_1$ it follows that $x_{Z1} = 359$ m (1177 ft); similarly, from Eqs. 8 and 10 $x_{Z2} = 456$ m (1496 ft) and $x_{Z3} = 891.5$ m (2925 ft). Shock wave Z_4Z_6 can be derived from Eq. 15 by letting $t = 2c = 150$ s so that $x_{Z4} = 1044$ m (4425 ft). Since q_1 and q_2 are assumed constant from cycle to cycle it follows that $t_{Z6} = t_M - 75 = 67$ s and $x_{Z6} = x_M = 1688$ m (5538 ft). Similarly x_{Z5} is obtained from Eq. 18 by letting $t = 3c = 225$ s, i.e., $x_{Z5} = 1767$ m (5796 ft).

Thus in Figure 5 at $t = 0 \equiv t_S$ traffic released during the three previous cycles is considered. The dashed line STT' represents the path of the

platoon head entering the link at $t = 0$, i.e., at the beginning of the effective green. This path was plotted on scale from Eq. 44 in which $t_T = 105$ s, $x_T = 1328.3$ m (4358 ft); t_T and x_T were computed from Eqs. 40 and 43 using $\alpha = 2.04$ (Eq. 41) and $\beta = 0.13$ (Eq. 42). In order to demonstrate an example of both dispersion and compression the platoon tail was arbitrarily selected as the mass of cars which enters the link at $t = 10$ s. It is reminded that the term platoon is loosely defined here as any arbitrarily selected group of vehicles. Line ABB' represents the trajectory of the platoon tail which is given from Eqs. 30 and 36; the coordinates of point B are obtained from Eqs. 31 and 32 which yield $t_B = 27$ s and $x_B = 160.3$ m (526 ft). Based on the information presented to this point Table V was prepared showing the position of the head and tail and the platoon length at discrete time points. As the table suggests, platoon length increases (i.e., platoon expands) up to $t = 100$ s. After this time the distance between head and tail begins to decrease, i.e., platoon is compressing. For further clarity the results of Table V are also shown graphically in Figure 7 from which the same conclusions can be drawn.

The phenomenon of platoon contraction and expansion can also be demonstrated by examination of the platoon's passage time defined as the time required for the entire platoon to cross a given point of the highway. Table VI shows the platoon passage time at a number of points downstream of the link; arrival times of the head were obtained from Eqs. 39 and 44 and for the tail from Eqs. 30 and 36. It is noted that at $x = 0$ passage time is 10 s. Inspection of Table VI suggests that passage time increases up to $x = 1219.2$ m (4000 ft) implying that platoon expands. After about this distance platoon compresses as passage time decreases. These results are consistent with those of Table V.

Flow rate variations at discrete points along the link was also studied based on the discussion of the previous sections. Referring again to Figure

TABLE V

Summary of Car Paths and Platoon Length for the Numerical Example

Time (s)	Position of Head in m (ft)	Position of Tail in m (ft)	Platoon Length $P_x(t)$ in m (ft)
0	0	0	0
10	126.5 (415)	0	126.5 (415)
20	253 (830)	97.2 (319)	155.8 (511)
40	506 (1660)	291 (955)	215 (705)
60	759 (2490)	504.1 (1654)	254.9 (836)
80	1011.9 (3320)	726 (2382)	285.9 (938)
100	1276.5 (4188)	953.1 (3127)	323.4 (1061)
120	1485.3 (4873)	1184.5 (3886)	300.8 (987)
140	1696.8 (5567)	1418.5 (4654)	278.3 (913)
160	1911.1 (6270)	1655.1 (5430)	256 (840)

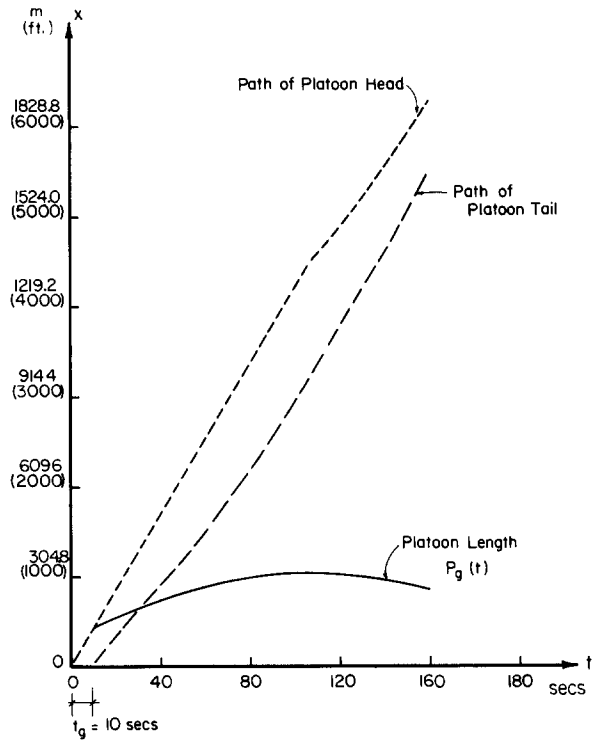

Fig. 7. Car paths and platoon length.

TABLE VI

Arrival Times of Platoon Head and Tail at Selected Points Along the Link

Distance m (ft)	Arrival Times		Passage Time (s)	Remarks
	Head	Tail		
152.4 (500)	12	26	14	—
304.8 (1000)	24	41	17	Expansion
609.6 (2000)	48	70	22	Expansion
914.4 (3000)	72	97	25	Expansion
1219.2 (4000)	96	123	27	Expansion
1524 (5000)	124	149	25	Contraction
1828.8 (6000)	153	174	21	Contraction

5 the three points selected were $x_1 = 304.8$ m (1000 ft), $x_2 = 914.4$ m (3000 ft) and $x_3 = 1828.8$ m (6000 ft). From Eqs. 71, 72, 74 and 76 it can be verified that $t_{S1} = 25.6$ s, $t_{S1'} = 50.2$ s, $t_{J1'} = 69$ s and $t_{J1} = 100.6$ s. Flow rate between t_{S1} and $t_{S1'}$ varies according to Eq. 70 while in the intervals $[t_{S1'}, t_{J1'}]$ and $[t_{J1'}, t_{J1}]$ it is 1045 veh/h (Eq. 73) and 283 veh/h (Eq. 75). Similarly, for $x_2 = 914.4$ m (3000 ft) $t_{S2} = 77$ s (Eq. 78), $t_{J2'} = 136$ s (Eq.

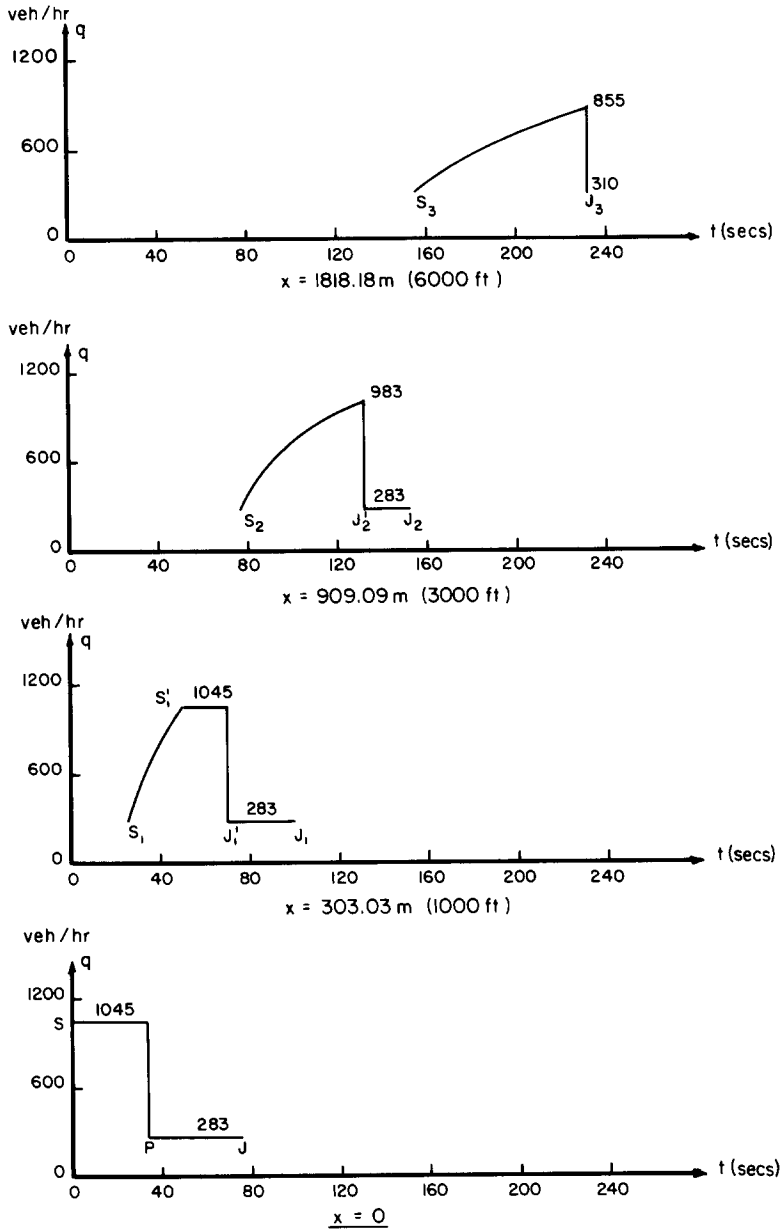

Fig. 8. Flow rates at representative distances along the link.

79), $t_{J2} = 152$ s (Eq. 81) and for $x_3 = 1828.8$ m (6000 ft) $t_{S3} = 156$ s (Eq. 83) and $t_{J3} = 231$ s (Eq. 84). From these results and using Eqs. 77 and 80 for calculating q along $S_2J_2'J_2$ (Fig. 5) and Eq. 81 for line S_3J_3 Figure 8 was drawn. This figure depicts flow rates at distances 0, 304.8 m (1000 ft), 914.4 m (3000 ft) and 1828.8 m (6000 ft) from the upstream end of the link due to the traffic released during the present cycle; at the steady state the same patterns are repeated periodically. Figure 8 suggests that flow rate patterns become smoother as distance increases, i.e., the effect of the traffic signal interruption becomes less pronounced eventually leading to uniform flows at very large distances.

CONCLUDING REMARKS

THE MODELING and the analysis of traffic dynamics at signalized links presented here appear to be reasonable and consistent with one's expectations especially at the moderate to high volume ranges in which shock waves will almost certainly be realized. Nonetheless, it must be recognized that the proposed models have not been tested as yet against field data. Testing is in fact intended in the future but before it is accomplished a more realistic flow-density relationship should be employed. Such relationship (or perhaps a number of them) tested and calibrated against actual data, should affect only the quantitative results presented in this study. However, the qualitative results (shock wave developments, compression, dispersion) should not be seriously affected. Naturally, analysis with a different flow-density model can be performed similarly and mathematical complexities can be surpassed by developing numerical solutions. It should be noted that the previous analysis did not take into account all possible shock wave developments. For example, referring to Figure 3 it is certainly possible that point Q occurs in the current rather than the next or perhaps two or more cycles later. Analysis for such details is identical and could not be included in this paper due to space limitations. Further improvements can be realized by adding stochastic elements to the basic modeling which can further be expanded to include traffic generators (or sinks) within the link.

Despite these shortcomings, the new concepts and results presented earlier (platoon compression, paths, etc.) should assist in better understanding the traffic dynamics at signalized links. To be sure, the concept of car paths in a traffic hump was also presented by Lighthill and Whitham,[7] however, no analytical expressions were developed while platoons, flow rates and traffic dynamics at signalized links were not considered. Discussions with practicing traffic analysts verified not only their awareness of platoon compression for some time but also their inability to describe this process mathematically. Finally, it is noted that

the car path equations are particularly important for developing an efficient coordination scheme as they can be used for more realistically predicting (in a macroscopic fashion) platoon arrival times at the downstream signal. Flow rate equations are also needed for control purposes for predicting the arrival patterns at the downstream signal. It should be remembered, however, that practical applications shall be attempted only following the improvements suggested earlier. These improvements will necessitate employment of numerical techniques.

ACKNOWLEDGMENTS

THE AUTHORS would like to acknowledge financial support from the Program of University Research of the U.S. Department of Transportation (Project DOT-RC-82008).

REFERENCES

1. T. V. EL-REEDY AND R. ASHWORTH, "Platoon Dispersion Along a Major Road in Sheffield," *Traf. Eng. Contr.* **19,** 186–189 (1978).
2. N. H. GARTNER, J. D. LITTLE AND H. GABBAY, "Optimization of Traffic Signal Settings by Mixed Integer Linear Programming; I. The Network Coordination Problem," *Trans. Sci.*, **9,** 321–343 (1975).
3. D. C. GAZIS, *Traffic Science*, pp. 175–241. Willey Interscience, New York, 1974.
4. D. L. GERLOUGH AND M. J. HUBER, *Traffic Flow Theory: A Monograph*, Trans. Res. Board, S.R. 156, Washington, D.C., 1975.
5. M. J. GRACE AND R. B. POTTS, "A Theory of Diffusion of Traffic Platoons," *Opns. Res.* **12,** 255–275 (1964).
6. B. D. GREENSHIELDS, "A Study of Traffic Capacity," *Proc. Hwy. Res. Board* **14,** 448–477 (1934).
7. M. H. LIGHTHILL AND G. B. WHITHAM, "On Kinematic Waves; II. A Theory of Traffic Flow on Long Crowded Roads," *Proc. R. Soc. Ser. A* **229,** 317–345 (1955).
8. P. G. MICHALOPOULOS, G. STEPHANOPOULOS AND V. B. PISHARODY, "Modeling of Traffic Flow at Signalized Links," *Trans. Sci.* **12,** 9–41 (1980).
9. Z. A. NEMETH AND R. L. VECELLIO, "Investigation of the Dynamics of Platoon Dispersion," *H.R.R. No. 334*, 23–33 (1970).
10. G. M. PACEY, "Progress of a Bunch of Vehicles Released from a Traffic Signal," Dept. of Scientific & Industrial Research, Road Research Laboratory, Report RN/2665, England, 1956.
11. D. I. ROBERTSON, "TRANSYT: A Traffic Network Study Tool," Road Research Laboratory, Report LR253, England, 1969.
12. P. A. SEDDON, "Another Look at Platoon Dispersion; 3. The Recurrence Relationship," *Traf. Eng. Contr.* **13,** 442–444 (1972).
13. G. STEPHANOPOULOS, P. G. MICHALOPOULOS AND G. STEPHANOPOULOS,

"Modelling and Analysis of Traffic Queue Dynamics at Signalized Intersections," *Trans. Res.* **13A,** 295–307 (1979).

14. F. V. WEBSTER, "Traffic Signal Settings," Road Research Laboratory, Paper No. 39, England, 1958.

(Received January 1980)